Thioamido Coordination in a Thioxo-1,2,4-triazole Copper(II) Complex Enhances Nonapoptotic Programmed Cell Death Associated with Copper Accumulation and Oxidative Stress in Human Cancer Cells

Saverio Tardito,[‡] Ovidio Bussolati,[‡] Monica Maffini,[†] Matteo Tegoni,[†] Marco Giannetto,[†] Valeria Dall'Asta,[‡] Renata Franchi-Gazzola,[‡] Maurizio Lanfranchi,[†] Maria Angela Pellinghelli,[†] Claudio Mucchino,[†] Giovanni Mori,[†] and Luciano Marchiò[†,*]

Dipartimento di Chimica Generale ed Inorganica, Chimica Analitica, Chimica Fisica, Università degli Studi di Parma, Viale G.P. Usberti 17/A, 43100 Parma, Italy, and Dipartimento di Medicina Sperimentale, Sezione di Patologia Generale e Clinica, Via Volturno 39, 43100 Parma, Italy

Received October 10, 2006

The thioamido function of $[CuCl_2(\mathbf{1}H)]Cl$ (**2**) (**1** = 4-amino-1,4-dihydro-3-(2-pyridyl)-5-thioxo-1,2,4-triazole), a cytotoxic copper complex, was converted into thioether moieties, leading to the synthesis of $[CuCl_2(\mathbf{3})]_2$ (**4**) and $[CuCl_2(\mathbf{5})]$ (**6**) (**3** = 6-methyl-3-pyridin-2-yl-7*H*-[1,2,4]triazolo[3,4-*b*][1,3,4]thiadiazine; **5** = 4-amino-5-ethylthio-3-(2-pyridyl)-1,2,4-triazole). These complexes were structurally characterized, and their stability constants, along with their biological activity, were determined. **4** and **6** were slightly less stable and significantly less active than **2**. However, as **2**, both complexes induced nonapoptotic vacuolar cell death. Copper uptake, investigated in both **2**-sensitive and -insensitive cell types, was markedly higher in sensitive cells where it was associated with an increase in oxidized glutathione. These data suggest that the thioamido function enhances the cytotoxicity of copper complexes in cancer cells promoting the accumulation of the metal and its interaction with cell thiols.

Introduction

The endogenous availability of copper and the strict regulation of its intracellular concentration[1,2] have stimulated the synthesis of copper-based drugs as potential anticancer compounds endowed with less severe side-effects than standard anticancer drugs.[3] Since copper is a redox active metal, the chemical processes that trigger its activity/toxicity have usually been associated with the generation of reactive oxygen species (ROS)[4] or with the alteration of the cellular oxidative status through glutathione (GSH) oxidation or depletion.[5] These properties may explain also the immunomodulatory activity of copper complexes, recently reported in vivo.[6,7] It is demonstrated that GSH protects cells through the stabilization of the cellular redox state and the detoxification of xenobiotics, thus modulating the efficacy of many anticancer drug.[8,9] Several Cu(II) complexes are based on the thiosemicarbazone moiety that displays the thioamido function for metal coordination.[10,11] Through the modification of the peripheral part of the ligands, a number of thiosemicarbazone derivatives were produced. Some of these complexes were tested in leukemia cell lines and found to exhibit antiproliferative activity referable to the triggering of apoptotic pathways.[12,13] Other Cu(II) compounds, based on polydentate nitrogen and oxygen donor ligands, showed ROS-related antiproliferative activity against tumor cells,[14] whereas other complexes were able to cleave DNA through the metal redox activity mediated by the ligand.[15] As far as the sulfur-containing ligands are concerned, it has been recently shown that the rich redox chemistry of the thione group[16] can confer interesting biological properties, as demonstrated by the chemopreventive agent oltipraz,[17] which seems to induce protective biological mechanisms through radical generation. Direct damage to DNA was instead demonstrated for the ROS generation elicited by the photochemical activation of *N*-hydroxypyridine-2-thione.[18,19] Thus, the combined redox activities of Cu(II) and the thione function can exert a synergic effect and underlie, at least in part, the antiproliferative properties of some Cu(II) complexes. Moreover, it was recently reported that copper complexes bearing a thioxo group showed strong toxicity against cancer cell lines or cancer xenografts.[20,21]

Our laboratory previously demonstrated that in HT1080 human fibrosarcoma cells, the thioxo-1,2,4-triazole copper(II) complex (**2**, Chart 1) exhibits a cytotoxic activity comparable to that demonstrated by cisplatin ($IC_{50} \approx 12\ \mu M$).[22] Interestingly, normal human fibroblasts (HF) were not sensitive to the cytotoxic effects of **2**. These effects were further investigated, leading to the conclusion that the drug, named A0 in that study, causes a variant of programmed cells death (PCD) clearly distinct from apoptosis.[23] Indeed, the morphological hallmark of the death process induced by **2** was found to consist of a massive cytoplasmic vacuolization, likely due to an enlargement of the endoplasmic reticulum, which eventually involved the whole cytoplasm. In the same contribution, the plasma membrane was preserved throughout the process, thus excluding an oncotic type of death, and no evidence of nuclear fragmentation was found, although a peripheral chromatin condensation was observed. More importantly, caspase-3 activation, a biochemical feature of apoptosis,[24,25] was not detectable upon the treatment with **2** that, rather, inhibited caspase-3 activation by cisplatin. This result suggests that **2** drives sensitive cells toward a nonapoptotic PCD because it blocks caspase-3-dependent apoptotic pathways.

To gain insight into the structure−activity relationship of **2**, we have modified the thioamido function of **1** (Chart 1) and we have evaluated the chemical properties and the cytotoxic activity of the newly synthesized complexes. In particular, the thioamido group of **1** was converted into a thioether (**3** and **5**,

* Corresponding author: Luciano Marchiò: Tel. +39 0521 905424; fax: +39 0521 905557; e-mail: marchio@unipr.it.

† Dipartimento di Chimica Generale ed Inorganica, Chimica Analitica, Chimica Fisica.

‡ Dipartimento di Medicina Sperimentale, Sezione di Patologia Generale e Clinica.

10.1021/jm061174f CCC: $37.00
Published on Web 03/21/2007

Chart 1. Molecular Structures of Ligands and Copper(II) Complexes

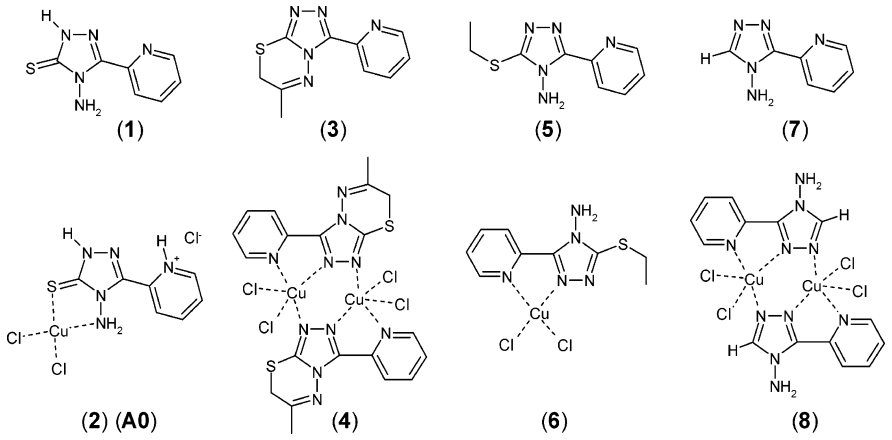

Chart 1) or completely desulfurated (**7**, Chart 1). The X-ray molecular structures of the complexes $[CuCl_2(\mathbf{7})]_2$ (**8**), **4** and **6** are reported (Figures 1−3) and the formation constants of **2**, **4**, and **6** in aqueous media were determined by means of spectrophotometric titrations, pointing to a slightly greater stability of **2** with respect to the other two complexes. We show here that these modifications result in a significant decrease in the biological activity of the new compounds, suggesting that the thioamido group is, at least in part, responsible for the cytotoxicity of **2**. However, the cytotoxic process activated by both **4** and **6** presents the same morphological features described in **2**-treated cells, indicating the activation of the same death pathway. To understand the mechanisms underlying the process, we have also evaluated ROS generation and the cell content of glutathione in HT1080 cells treated with **2,** along with copper uptake in sensitive and insensitive cell types.

Results and Discussion

Spontaneous Desulfuration of 2. The development of novel metal anticancer drugs is stimulated by the need for compounds endowed with cytotoxic mechanisms alternative and/or complementary to those of current drugs.[26,27] Thus, the comprehension of the mechanism of action of a chemotherapeutic agent is of crucial importance for the definition of its therapeutic potential. Moreover, it can suggest structural modifications leading to compounds with enhanced activity.[28] For these reasons, given the marked cytotoxic activity of **2**,[22] we have investigated other complexes in which the ligands were designed with specific modifications of **1**.[29]

We reasoned that the coordination properties of the thioamide function of **1** can provide stability to **2**. At the same time, the thioamide function can be the source of redox activity since, in the presence of redox active metal ions, it is subjected to successive oxidation steps that ultimately lead to the desulfuration of the ligand.[16] In fact, clear green DMSO solutions or HCl-acidified water solutions (pH ≈ 3.8) of **2** (2 mM), kept at room temperature, show the presence of a pale green precipitate after few weeks. This precipitate was collected and crystallized from DMSO or HCl_{conc} solutions, respectively. The X-ray analysis of the crystals obtained from the two solvents revealed that the complex **8** exhibits the same dinuclear structure (Chart 1 and Figure 1). It is evident that the ligand is desulfurated, and this can be the result of the Cu(II)/Cu(I) redox cycling associated with the redox activity of the thioamido group. Similar partial or complete desulfuration processes were reported

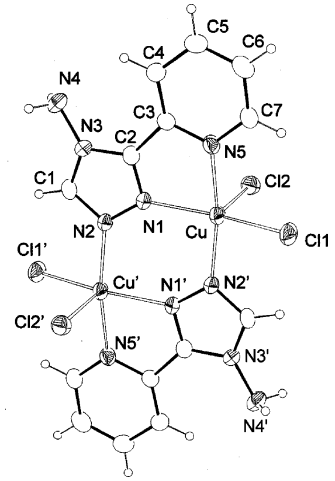

Figure 1. ORTEP drawing of **8** at the 30% thermal ellipsoids level. Cu−N(1) = 2.050(4) Å, Cu−N(2) = 1.996(4) Å, Cu−N(5) = 2.045(4) Å, Cu−Cl(1) = 2.270(1) Å, Cu−Cl(2) = 2.463(2) Å. (′) = 1 − *x*; −*y*; 1 − *z*.

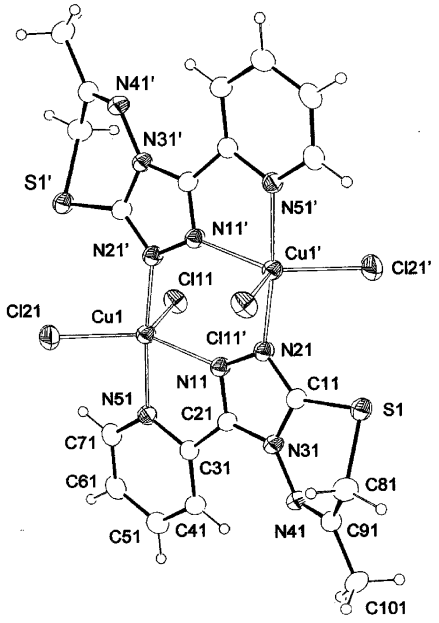

Figure 2. ORTEP drawing of one of the molecular unit of **4** at the 30% thermal ellipsoids level. Cu(1)−N(11) = 2.133(3) Å, Cu(1)−N(21)′ = 1.992(3) Å, Cu(1)−N(51) = 2.004(3) Å, Cu(1)−Cl(11) = 2.400(1) Å, Cu(1)−Cl(21) = 2.257(1) Å, ‘ = −*x*; −*y*; −*z*. The second molecular unit presents the following geometric parameters: Cu(2)−N(12) = 2.168(3) Å, Cu(2)−N(22)″ = 1.992(3) Å, Cu(2)−N(52) = 2.025(3) Å, Cu(2)−Cl(12) = 2.312(1) Å, Cu(2)−Cl(22)= 2.290(1) Å. (″) = 1 − *x*; −*y*; 1 − *z*.

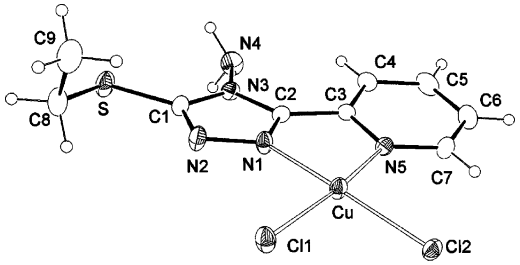

Figure 3. ORTEP drawing of **6** at the 30% thermal ellipsoids level. Cu−N(1) = 1.999(3) Å, Cu−N(5) = 2.098(3) Å, Cu−Cl(1) = 2.255(1) Å, Cu−Cl(2) = 2.273(1) Å.

Scheme 1. Desulfuration Reactions of **2**

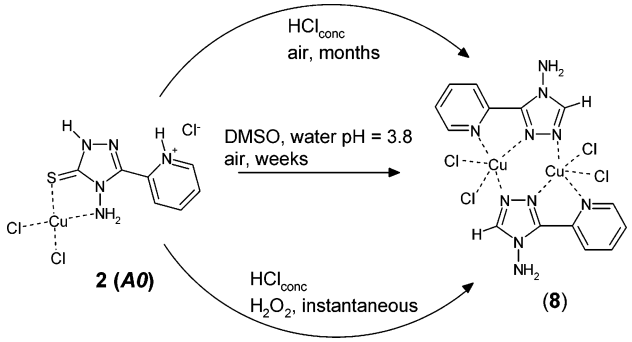

for copper(II) complexes exhibiting thioamido groups in which the desulfuration was achieved through mild oxidative agents[30] or basic media.[31,32,16] The desulfuration process does not usually occur in acidic media. However, it is interesting to note that, also in HCl_{conc} solutions of **2** exposed to air for few months, green crystals of **8** formed on the solution surface. An analogous phenomenon was previously reported for a similar sulfurated triazole copper complex.[33] Nevertheless, **2** can be dissolved in HCl_{conc} and stored under nitrogen for an unlimited time without the occurrence of any desulfuration phenomena. This observation demonstrates that air oxygen mediates the redox processes. The complex **8** can be obtained also from HCl_{conc} solution of **2** after treatment with H_2O_2. In this case, the reaction is instantaneous and bright green crystals of **8** can be isolated in few hours. These redox processes are summarized in Scheme 1. The importance of the thioamido function for the activity of **2** is evidenced by the fact that DMSO or HCl acidified water solutions of the complex exhibit decreasing cytotoxic activity as a function of time (results not shown).

Synthesis and Description of the Molecular Structures of (4)·3/2H$_2$O, 6, and 8. To test further the hypothesis that the thioamido function is important for the biological activity of **2**, **1** was converted into **3**, using chloroacetone in absolute ethanol, or in **5**, using ethyl iodide/NaOH in dimethylformamide. The corresponding copper(II) complexes **4** and **6** were prepared. The structural features of **4** are analogous to those of **8** since the thioamido group was converted into a thioether that presents less coordination ability, whereas **6** presents a mononuclear structure with the ligand N,N bound as a consequence of the steric hindrance on the thioether group, as described in Chart 1 and Figures 1−3.

The dinuclear complexes **4** and **8** are centrosymmetric, and, in both compounds, each copper is bound by two triazoline nitrogen atoms, a pyridine nitrogen atom, and two chlorine ions, Figure 1 and 2. In **8** the metals adopt a square pyramidal geometry with the apical Cu−Cl(2) bond distance significantly longer (2.463(2) Å) than the equatorial one (Cu−Cl(1): 2.270(1) Å). In the unit cell of **4,** two independent molecular units are present that exhibit a trigonal pyramidal geometry with the apical position occupied by N(51) and N(21) for unit 1 and N(52) and N(22) for unit 2. However, for unit 1 the Cu−Cl distances are essentially equivalent (2.312(1) and 2.290(1) Å), whereas for unit 2 they differ significantly (2.257(1) and 2.400(1) Å) pointing to a certain degree of distortion toward the square pyramidal geometry. In addition, the two units of **4** differ also in the envelope conformation of the hexacyclic thiadiazine ring. The Cu−N bond distances of **8** are in the range 1.996(4)−2.050(4) whereas in **4** the Cu−N bond length in the equatorial position is significantly longer (2.133(3) Å for Cu(1) and 2.168(3) Å for Cu(2)) than the apical Cu−N bond distances (range: 1.992(3)−2.025(3) Å). For both compounds, the ligands act as κ^3-N,N′,N″ donors, and, specifically, they chelate with the pyridine nitrogen atom and the endocyclic N(1) triazoline atom while bridging to a second metal center with the vicinal endocyclic N(2) atom. The distance between the two metals is 4.126(1) Å in **8** and 4.223(2)−4.228(2) Å in **4**. The molecular structure of **6** is reported in Figure 3. The metal adopts a square pyramidal geometry bound by two chlorines and the κ^2-N,N′ chelate ligand. The steric hindrance of the ethyl group of the thioether function hinders the N(2) nitrogen atoms that becomes unavailable for the metal coordination. This precludes the formation of a dinuclear structure as in the case of the **4** and **8** complexes.

Solution Studies of Copper Complexes. The complex formation of **2** was studied by means of spectrophotometric titration of a Cu(II) solution with a solution of **1** acidified by HNO_3. Nitric acid was used instead of HCl, as precipitation occurred in presence of high concentration of chloride ions. For the same reason, no supporting electrolyte was used in order to exclude complex precipitation. Refinement of the spectroscopic data led to the determination of the log K of both a 1:1 and a 1:2 M:ligand species (log K_1 = 5.4(1) and log K_2 = 9.1(4)). As the calculated pH ranged from 1.34 to 2.86 during the titration, both the $[Cu(\mathbf{1}H)]^{3+}$ and $[Cu(\mathbf{1})]^{2+}$ species were formed, which differ only by the protonation of the peripheral pyridyl substituent,[34] Chart 1. Thus, the log K_1 of 5.4(1) can be associated with both the Cu(II) + $\mathbf{1}H^+$ = $[Cu(\mathbf{1}H)]^{3+}$ and Cu(II) + **1** = $[Cu(\mathbf{1}H)]^{2+}$ equilibria. This constant value is correlated to the stability of the S,N coordination of the thioxotriazole to Cu(II). The log K_2 = 9.1(4) was attributed to the formation of the $[Cu(\mathbf{1}H)_2]^{4+}$ and $[Cu(\mathbf{1})_2]^{2+}$, which were not isolated in the solid state but exist in solution in the presence of an excess of **1** ligand.

The speciation models determined in aqueous solution (T = 25 °C, I = 0.1 M (KCl)) for both the Cu(II)/**3** and Cu(II)/**5** systems consist of 1:1 and 1:2 species. The log β values are 4.75(4) and 9.72(5) for $[Cu(\mathbf{3})]^{2+}$ and $[Cu(\mathbf{3})_2]^{2+}$, and 4.89(5) and 9.84(9) for $[Cu(\mathbf{5})]^{2+}$ and $[Cu(\mathbf{5})_2]^{2+}$. It is noteworthy that for **3**, the inclusion of the dinuclear $[Cu(\mathbf{3})]_2^{4+}$ species in the speciation model (according to the X-ray structure) resulted in its rejection and, when considered in place of the $[Cu(\mathbf{3})]^{2+}$ species, it led to significantly higher sample standard deviations and poor fitting of the spectrophotometric data. It is reasonable to assume that, in aqueous solution, the complex **4** exhibits a mononuclear structure as a result of the coordination capability of water. This data would be in accordance with the analogous behavior of **6**.

Determination of Cytotoxic Activity of 4 and 6 Complexes. The cytotoxic activities of **4** and **6** were evaluated on the HT1080 cell line with the resazurin assay. In these experiments, cells were incubated for 48 h with increasing concentrations of the complexes (5−300 μM). Dose−response curves are reported

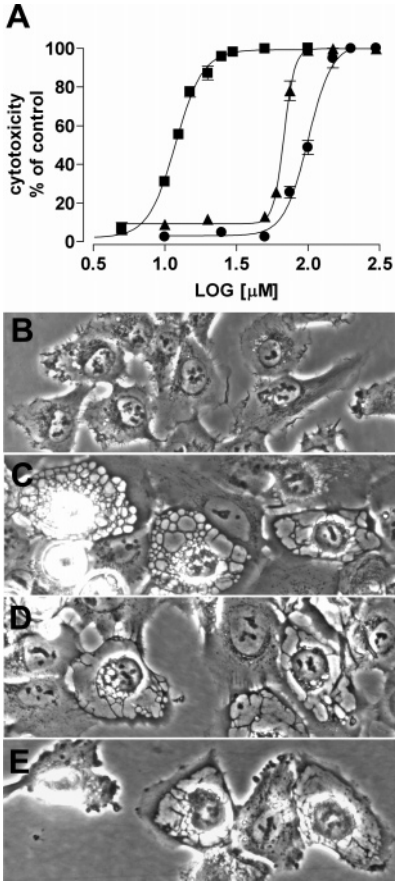

Figure 4. (A) Dose−response curves obtained after a 48 h incubation of HT1080 cells with the indicated concentrations of **2** (■), **4** (●), and **6** (▲). Data are means of six independent determinations with SEM shown when greater than the size of the point. (B−E) Phase contrast images of HT1080 cells: untreated (B), treated for 24 h with 25 μM of **2** (C), treated for 24 h with 150 μM **4** (D) and treated for 24 h with 75 μM **6** (D). Note the extensive cytoplasmic vacuolization in treated cells (original magnification ×400).

in Figure 4. Unfortunately, the limited solubility of **8** in water or DMSO did not allow the evaluation of the dose−response curve for this complex. The results indicate that **2** is endowed with a significantly greater potency than the other complexes. It is noteworthy that the slopes of the three dose−response curves obtained are similarly very steep, thus suggesting that a threshold concentration must be reached before a relatively sharp increase in cytotoxicity is achieved. The IC_{50} of **4** is 100 μM and that of **6** is 68 μM (Figure 4A), considerably higher than the value calculated under the same conditions for **2** ($IC_{50} \sim$ 12 μM).[22] Nevertheless, the morphological analysis shown in Figure 4B−E demonstrates that all the complexes trigger the same cytotoxic response. The endoplasmic reticulum swells, leading to an extensive cytoplasmic vacuolization, which is consistent with Clarke's type III of programmed cell death,[35] as originally proposed for cell death induced by **2** by our group.[23] The presence of a massive cytoplasmic vacuolization in the dying cells treated with all the triazole copper complexes tested here definitely discriminates this form of toxicity from other modalities of nonapoptotic PCD, such as necroptosis.[36]

Correlation between 2 Sensitivity and Copper Uptake in Human Cells. To investigate the mechanism(s) underlying the cytotoxic activity induced by thioxotriazole copper complexes, we have assayed the viability of two tumor cell lines, HeLa and SW872 cells, as well as of human normal fibroblasts, treated for 48 h with concentrations of **2** ranging from 5 to 50 μM

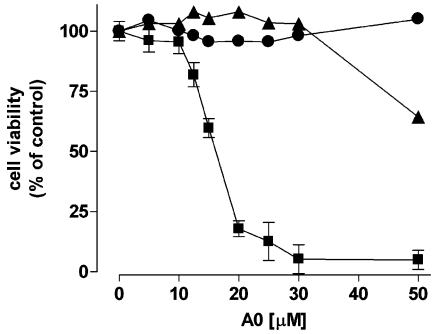

Figure 5. Cell viability in human cells treated with **2**. HeLa cells (■), SW872 cells (▲), and human fibroblasts (●) were treated with the indicated concentrations of **2** for 48 h. Cell viability, expressed as percent of fluorescence values obtained for untreated cells, was measured with the resazurin assay. Data are means of six independent determinations with SEM shown when greater than the size of the point.

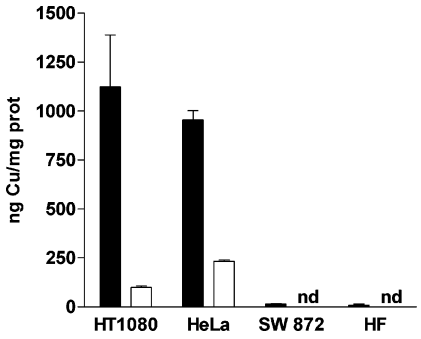

Figure 6. Cell content of copper in cultured cells: effect of **2**. Copper content was measured (see Experimental Section) in extracts of the indicated cell lines incubated for 12 h with 25 μM of **2** (black bars) or 25 μM of CuCl2 (white bars). 1−1.5 × 107 cells, roughly corresponding to 4−9 mg of total cell proteins, were used for each condition. Data are means of three independent determinations with SD shown.

(Figure 5). The cytotoxicity induced by **2** in HeLa cells was comparable to that observed in HT1080 cultures, with a slightly smaller sensitivity (IC_{50} = 16 μM). Also HeLa cells exhibited the same vacuolization process previously observed in HT1080 cells (data not shown). Conversely, the proliferation of SW872 cells was only partially compromised even by the highest concentration used for **2**, and no appreciable cytotoxic change was observed. The viability of human fibroblasts was unaffected by **2** in the whole concentration range adopted.

Assuming the greater stability determined for **2**, we wondered if the different cell sensitivity to **2** may involve the amount of copper accumulated by the cells during the treatment with the complex. To investigate this possibility, cell uptake of copper was determined after a 12 h incubation with **2** or $CuCl_2$, both at 25 μM, on the same cell lines used for the viability data (HeLa, SW872, HT1080, and HF), Figure 6. After 12 h of treatment with **2**, the sensitive cell lines HT1080 and HeLa had cell copper contents at least 1000-fold higher than untreated, control cells, which had a copper content below the sensitivity of the method used (>0.8 ng Cu/mg prot). Under the same conditions, the incubation of HT1080 and HeLa cells with $CuCl_2$ led to a copper accumulation lower by 90% and 80%, respectively, compared to **2**-treated cells. In contrast, in the **2**-insensitive SW872 cells and HF the copper accumulation after the treatment with the complex was very low, while it was below the sensitivity of the method after exposure to $CuCl_2$. These results indicate that sensitive cells tend to accumulate more copper than insensitive cells and that **2** greatly favors the intracellular accumulation of the metal. Although the cell panel

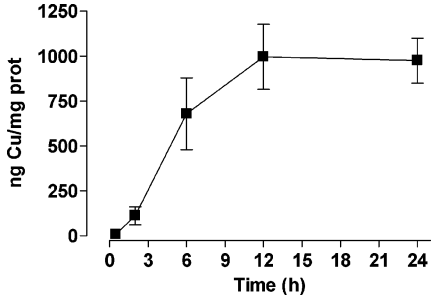

Figure 7. Time-course of copper uptake in **2**-treated HT1080 cells. Cells were incubated for 24 h in the presence of 25 μM of **2**. Cell subcultures were extracted at the indicated times and copper content was determined as described in Experimental Section. Data are means of three independent determinations with SD shown.

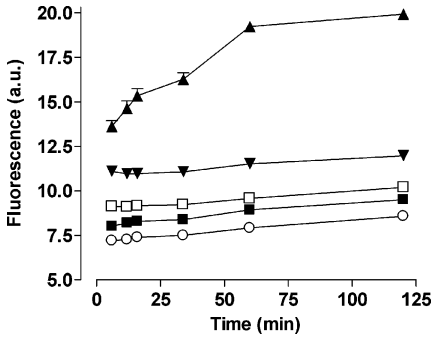

Figure 8. Effect of **2** on ROS generation in a cell-free system. H_2DCFDA was deesterified with NaOH and then dissolved at a concentration of 10 μM in complete growth medium in the absence (○, control) or in the presence of $CuCl_2/H_2O_2$ (25 μM/100 μM, ▲), H_2O_2 (100 μM, ▼), **2** (25 μM, □), $CuCl_2$ (25 μM, ■). Data are means of six independent determinations with SD shown when greater than the size of the point. A representative experiment, repeated three times with comparable results, is shown.

investigated here is small, it is evident that the sensitivity to **2** correlates with the amount of copper taken up by cells upon treatment with **2**, pointing to a cell specific balance between influx and efflux as a possible sensitivity marker.

In Figure 7 the time course of copper uptake in HT1080 cells is presented. The accumulation is clearly time dependent for several hours and, after a relatively steep increase during the first 6 h, it reaches a plateau after 12 h of treatment and stabilizes thereafter. Interestingly, this time point roughly corresponds to the appearance of the peculiar cytoplasmic vacuoles that characterize **2**-induced death.

Markers of Oxidative Stress during Treatment with Complex 2. To assess if the cytotoxic effects of **2** are mediated by the generation of ROS, we investigated the ability of **2** to oxidate the ROS-reactive fluorescent probe H_2DCFDA (2′,7′-dichlorodihydrofluorescein diacetate) in a cell-free system constituted by the cell growth medium. We compared the ability of **2** to generate ROS with that of known ROS-inducers such as H_2O_2, $CuCl_2$ and, in particular, $Cu(II)/H_2O_2$ that is able to sustain a Fenton-like redox cycle. The results (Figure 8) indicate that **2** was able to induce ROS to an extent comparable to that of $CuCl_2$, which, however, was only slightly greater than the basal fluorescence, obtained for the growth medium alone. Hydrogen peroxide alone increased the fluorescence 1.5 fold with respect to the control. Given the slight increase of fluorescence during the exposure (up to 120 min) to $CuCl_2$, H_2O_2, or **2**, it can be speculated that there was no significant production of ROS through redox cycles. In contrast, Fenton-like cycles generated by the $Cu(II)/H_2O_2$ system led to a

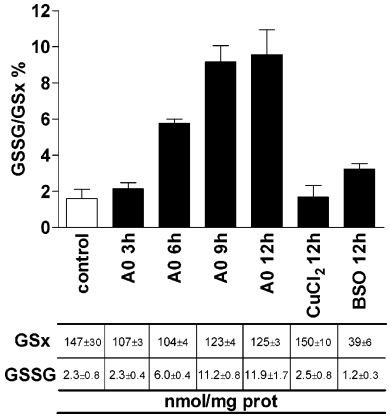

Figure 9. Oxidized (GSSG) and total (GSx) glutathione content and percent ratio in HT1080 cells. Untreated cells (control, white bar); cells treated for the indicated times with 25 μM of **2**, 25 μM $CuCl_2$, or 200 μM of buthionine sulfoximine (BSO) (black bars). The values of GSx and GSSG cell contents, in the same conditions indicated for bars, are expressed as nmol/mg of protein, are reported in the lower panel.

progressive time dependent increase of the fluorescence, which was 2.5 fold greater than the control after 1 h of reaction.

The ability of the same compounds to stimulate intracellular ROS production was investigated in the HT1080 cells with the H_2DCFDA probe, which detects water soluble ROS, and with the lipophilic fluorescent C11-BODIPY (4,4-difluoro-5-(4-phenyl-1,3-butadienyl)-4-bora-3a,4a-diaza-s-indacene-3-undecanoic acid) probe that, instead, is sensitive to lipid peroxidation. With both probes no appreciable increase in fluorescence was detected for **2**, $CuCl_2$, H_2O_2, or $Cu(II)/H_2O_2$. Comparable negative results with the same probes were obtained in another cell model by other authors.[37] The possible generation of ROS by **2** inside the cells remains to be explored with alternative techniques.

The most relevant nonenzymatic antioxidant that maintains the intracellular oxidative equilibrium is the tripeptide glutathione (Gly-Cys-γGlu). The GSx (total glutathione) and GSSG (oxidized glutathione) content of HT1080 cells treated with **2**, $CuCl_2$, or buthionine sulfoximine (BSO) for 3, 6, 9, 12 h is shown in Figure 9. In the first 6 h of treatment with 25 μM **2**, when the copper uptake mediated by the complex rises steadily (see Figure 7), GSx slightly decreases while GSSG markedly increases (lower panel). After 9 h of incubation, GSx content is nearly restored to control values (untreated cells), presumably as a consequence of the cell response to an oxidative injury through the upregulation of the glutathione synthase and/or glutathione reductase.[38] However, the amount of GSSG increases in a time-dependent fashion that roughly parallels the progressive accumulation of copper (see Figure 7), reaching a plateau at approximately 10% of GSSG between 9 and 12 h (Figure 9, upper panel). This behavior can be explained by assuming that the copper(II) is reduced to copper(I) by the reduced form GSH and then accumulated in the cells as a copper-GS adduct. The plateau value is 5-fold higher than the value obtained in control, untreated cells. $CuCl_2$ does not cause any significant change in GSx and GSSG levels compared to untreated cells. As a positive control, BSO, a specific inhibitor of GSH synthesis through γ-glutamyl synthase,[39] causes a drastic decrease of GSx. These results are consistent with data obtained by ionic exchange HPLC analysis of primary amine performed on the cell lysate of untreated and **2** treated cells (25 μM, 12 h). The chromatograms of **2**-treated cells exhibit a single peak difference with respect to that of untreated cells. This peak corresponds to the marked increase in GSSG due to **2** treatment (Figure S1 of

Supporting Information). Both methodologies yield comparable values of cell GSSG (data not shown).

From these results we propose that glutathione is one of the cellular targets of **2**, suggesting that the cells treated with the Cu(II) complex undergo a peculiar form of oxidative stress, which eventually triggers the vacuole-prone nonapoptotic cell death, possibly through the oxidative inhibition of caspase-3.[23] Interestingly, literature evidence reports other nonmetal agents that are responsible for caspase-3 inhibition through the oxidation of cell thiols and induce vacuolar cell death induction.[40]

Conclusions

The thioamido function of **1** has been modified so as to assess its role for the cytotoxic activity of the copper complex. The resulting Cu(II) thioether complexes **4** and **6** are less stable and have a reduced cytotoxic potency (IC_{50} of 100 and 68 μM in HT1080 cells, respectively, compared with 12 μM for **2**). However, these complexes also trigger the same peculiar type of cell death observed in **2**-treated cells, hallmarked by an extensive cytoplasmic vacuolization in the absence of apoptotic or oncotic features. Although many metal complexes have been synthesized and tested for antiproliferative activity,[41] to our knowledge there are no examples of compounds able to induce cytotoxic effects similar to those observed for these triazole compounds. HT1080 fibrosarcoma cells and HeLa cells exhibit a marked sensitivity to **2**, while normal human fibroblasts and SW872 liposarcoma cells were substantially insensitive to the complex. The sensitivity to **2** appeared to be correlated with the ability of the complex to facilitate copper accumulation in the cells, which, in turn, may be related to the enhanced stability of **2** conferred by the thioamido coordination. HT1080 and HeLa cells, indeed, showed a massive accumulation of copper after 12 h of exposure to **2**, when SW872 cells and human fibroblasts had barely detectable intracellular metal. In **2**-treated HT1080 cells, copper uptake is paralleled by an evident perturbation of the cell oxidative status, as indicated by a 5-fold increase of the oxidized form of glutathione, pointing to an interaction of the metal with cell thiols. As previously reported by our group, the activity of caspase-3, a protease with two cysteine residues sensitive to oxidation in its active site, is inhibited by **2**. However, the increase in oxidized glutathione should not be attributed to the generation of ROS by **2**, since the complex seems unable to increase ROS in a cell free system. In summary, we conclude that the **2**-thioamido function favors cell copper accumulation and, hence, metal driven oxidation of cell thiols critical for the survival of cancer cells.

Experimental Section

General Methods. The compound A0 (**2**) was prepared as previously reported.[22] All other reagents were commercially available (Sigma-Aldrich) and were used as received. Mass spectra were obtained with a Micromass ZMD spectrometer. The mixtures were analyzed in negative and positive ionization modes by direct perfusion in ESI-MS interface; capillary = 3.0 kV; cone = 20−70 V; extractor = 3 V. Infrared spectra were recorded on a Perkin-Elmer FT-IR Nexus spectrometer equipped with a microscope accessory. The IR data was collected in reflectance mode (4000 to 600 cm^{-1}) analyzing a small quantity of samples deposited on thin layers of alumina. Elemental analyses (C, H, N) were performed with a Carlo Erba EA 1108 automated analyzer.

Synthesis of 6-Methyl-3-(pyridin-2-yl)-7*H*- [1,2,4]triazolo[3,4-*b*][1,3,4]thiadiazine (3). Chloroacetone (1.3 mL, 16.1 mmol) was added to a suspension of **1** (3.0 g, 15.5 mmol) in 60 mL of absolute ethanol. The initially brown solution formed a yellow precipitate after 30 min. The mixture was stirred under reflux conditions for 4 h and then neutralized with aqueous Na_2CO_3 (1 M). The white precipitate was filtered off, and the brown solution was vacuum-dried. The brown solid was extracted in ethanol (3 × 20 mL), the solution was vacuum-dried, and the brown product was collected (3.1 g, 86%). Anal. ($C_{10}H_9N_5S$) C, H, N. Mass spectrum ESI-MS (MeOH) *m/z* (%): 231 (100, L^+) IR data (KBr disk, cm^{-1}): 3059w, 2967m, 2911m, 1587m, 1446s, 1431s, 1416s, 1289m, 974m, 787s. ^1H NMR (300 MHz, DMSO-d_6): 2.31 ppm (s, 3H, CH_3), 3.87 ppm (s, 2H, CH_2), 7.54 ppm (m, 1H, Py), 7.96 ppm (m, 2H, Py), 8.74 ppm (m, 1H, Py).

Synthesis of 4-Amino-5-ethylthio-3-(2-pyridyl)-1,2,4-triazole (5). 1 (0.40 g, 2.12 mmol) was dissolved in dimethylformamide (15 mL) and NaOH (0.09 g, 2.25 mmol). The green solution turns blue after the addition of ethyl iodide (0.17 mL, 2.12 mmol). The solution was then stirred for 5 h giving a red suspension. Water (40 mL) was added to the mixture, which was extracted with dichloromethane (4 × 20 mL) in a separatory funnel. The organic phase was washed with a 5% aqueous sodium thiosulfate solution (40 mL) and brine (40 mL), dried with anhydrous Na_2SO_4, filtered, and vacuum-dried, and the product was collected (0.27 g, 1.22 mmol, 61%). Anal. ($C_9H_{11}N_5S$) C, H, N. Mass spectrum ESI-MS (MeOH) *m/z* (%): 221 (100, LH^+) IR data (cm^{-1}): 3250s, 3145s, 3078m, 2959m, 2928m, 1638s, 1591s, 1471s, 1457s, 1152m, 1022s, 960m, 782m. ^1H NMR (300 MHz, $CDCl_3$): 1.49 ppm (t, 7.5 Hz, 3H, CH_3), 3.33 ppm (q, 7.5 Hz, 2H, CH_2), 6.21 ppm (s, 2H, NH_2), 7.38 ppm (m, 1H, Py), 7.87 ppm (m, 1H, Py), 8.31 ppm (d, 9.0 H Z,1H, Py), 8.62 ppm (d, 1.4 Hz, 1H, Py).

Synthesis of $[CuCl_2(3)]_2$ (4). In a round-bottom flask, an ethanolic solution (10 mL) of $CuCl_2 \cdot 2H_2O$ (0.183 g, 1.07 mmol) was added to a suspension of **3** (0.248 g, 1.07 mmol) in the same solvent (10 mL) and a dark green precipitate instantly formed. The suspension was acidified with 3 M HCl to pH 2 and refluxed for 2 h. The light green precipitate was filtered and collected. (0.382 g, 95%). Anal. ($C_{20}H_{18}Cl_4Cu_2N_{10}S_2$) C, H, N. ESI-MS (MeOH) m/z (%): 560.2 (100, $[CuCl(\mathbf{3})_2]^+$), 525.2 (20, $[Cu(\mathbf{3})_2]^+$), 329.0 (27, $[CuCl(\mathbf{3})]^+$), 262.6 (45, $[CuCl(\mathbf{3})]^{2+}$), positive ion mode. IR data (KBr disk, cm^{-1}): 3098w, 3052m, 2980m, 2947m, 1606m, 1489s, 1458s, 1420s, 1288m, 792m. Suitable crystals for X-ray structure analysis were grown from a HCl concd/water (1:1) solution.

Synthesis of $[CuCl_2(5)]$ (6). In a round-bottom flask, an ethanolic solution (20 mL) of $CuCl_2 \cdot 2H_2O$ (0.208 g, 1.22 mmol) was added to a solution of **5** (0.270 g, 1.22 mmol) in the same solvent (20 mL) and a green precipitate instantly formed. The suspension was stirred for 2 h, and the light green precipitate was filtered and collected. (0.321 g, 74%). Anal. ($C_9H_{11}Cl_2CuN_5S$) C, H, N. ESI-MS (MeOH) *m/z* (%): 540.3 (33, $[CuCl(\mathbf{5})_2]^+$), 505.3 (23, $[Cu(\mathbf{5})_2]^+$), 319.1 (60, $[CuCl(\mathbf{5})]^+$), positive ion mode. IR data (cm^{-1}): 3260s, 3183s, 3093w, 2984m, 1621s, 1605s, 1531m, 1507s, 1459s, 1396s, 1264m, 783m. Suitable crystals for X-ray structure analysis were grown by slow evaporation from a HCl concd/water (1:1) solution.

Synthesis of $[CuCl_2(7)]_2$ (8). In a round-bottom flask, 0.130 g of **2** (0.357 mmol) was dissolved with 5 mL of hot HCl_{conc}, giving a brown-green solution. A few drops of 30% H_2O_2 were added, which caused the solution color to change immediately to bright green. After a few days, a green crystalline material formed, which was filtered, washed with water, and collected (yield 0.072 g, 68%). Anal. ($C_{14}H_{14}Cl_4Cu_2N_{10}$) C, H, N. ESI-MS ($CH_3CN$/MeOH 1/1) *m/z* (%): 689.8 (4, $[Cu_3Cl_5(\mathbf{7})_2]^+$), 554.9 (7, $[Cu_2(\mathbf{7})_2Cl_3]^+$) 420.1 (65, $[CuCl(\mathbf{7})_2]^+$) 258.9 (100, $[CuCl(\mathbf{7})]^+$). IR (KBr pellets): 3271 s, 3200 s, 3124 s, 3057m, 3038m, 1640 s, 1608 s, 1521 s, 1469 s, 1431 s, 1333m, 1294 s, 1096 s, 818m, 805m, 703m cm^{-1}.

X-ray Crystallography. A summary of data collection and structure refinement for (**4**)·3/2H_2O, **6**, and **8** is reported in Table 1. Single-crystal data were collected with an Enraf Nonius CAD4 diffractometer (Cu Kα: λ = 1.54183 Å) for (**4**)·3/2H_2O and **8** and with a Philips PW 1100 diffractometer (Mo Kα; λ = 0.71073 Å) (**6**). Cell constants were obtained by a least-square refinement of the setting angles of 24 randomly distributed and carefully centered reflections. No crystal decay was observed for any compound. Absorption correction was applied using the method of Walker and

Table 1. Summary of X-ray Crystallographic Data for (**4**)·3/2H_2O, **6**, and **8**

empirical formula	$C_{20}H_{21}Cl_4Cu_2N_{10}O_{1.5}S_2$	$C_9H_{11}Cl_2CuN_5S$	$C_{14}H_{14}Cl_4Cu_2N_{10}$
formula weight	758.47	355.73	591.23
color, habit	green, block	green, prism	green, block
crystal size, mm	0.38 × 0.21 × 0.20	0.30 × 0.25 × 0.20	0.30 × 0.15 × 0.15
crystal system	triclinic	triclinic	monoclinic
space group	$P\bar{1}$	$P\bar{1}$	$P2_1/a$
a, Å	8.827(2)	8.649(3)	8.346(1)
b, Å	10.796(5)	9.313(5)	14.280(4)
c, Å	16.590(8)	9.371(4)	8.376(3)
α, deg	72.92(2)	68.69(2)	90
β, deg	85.50(2)	71.86(2)	93.43(2)
γ, deg	66.58(2)	79.27(2)	90
V, Å^3	1385(1)	666.0(5)	996.5(5)
Z	2	2	2
T, K	293	293	293
ρ(calc), mg/m^3	1.818	1.774	1.970
μ, mm^{-1}	7.195	2.185	7.807
θ range, deg	4.66 to 69.91	3.11 to 26.99	6.13 to 70.01
no.of rflcn/obsv	5208/4550	3254/1933	2007/1043
GooF	1.039	1.009	0.997
*R*1	0.0427	0.0390	0.0375
*wR*2	0.1142	0.0610	0.0523

$R1 = \Sigma||F_o| - |F_c||/\Sigma|F_o|$, $wR2 = [\Sigma[w(F_o^2 - F_c^2)^2]/\Sigma[w(F_o^2)^2]]^{1/2}$, $w = 1/[\sigma^2(F_o^2) + (aP)^2 + bP]$, where $P = [\max(F_o^2,0) + 2F_c^2]/3$.

Stuart[42] for (**4**) 3/2H_2O and **8** (min. and max. transmission factor of 0.783−1.000 and 0.862−1.000, respectively). The structures were solved by direct methods (SIR97)[43] and refined with full-matrix least-squares (SHELXL-97),[44] using the Wingx software package.[45] Nonhydrogen atoms were refined anisotropically; the NH_2 hydrogen atoms of **6** and **8** were found and refined whereas the remaining hydrogen atoms were placed at their calculated positions. Ortep diagrams were prepared using the ORTEP-3 for Windows program.[46]

Stability Constants Determination. Stock solutions of $CuCl_2$, **1**, **3**, and **5** were prepared by weight. To solubilize the ligand, the suspension of **1** (1.9×10^{-3} M) was acidified to pH ca. 1 by adding a proper amount of concd HNO_3. The titer of the $CuCl_2$ solution was checked by standard EDTA solution. KOH and HCl aqueous solutions (0.2 M) were prepared by diluting concentrated Merck Titrisol ampoules and standardized with the usual procedure of this laboratory.[47] The spectrophotometric titrations were carried out at $T = 25 \pm 0.1$ °C under a stream of N_2, using 50 cm^3 samples. Absorption spectra in the visible range (400−800 nm) were recorded with a Perkin-Elmer Lambda 25 spectrophotometer using matched quartz cells of 5 cm path length. Solutions were passed from the potentiometric vessel to the thermostated cuvette by means of a peristaltic pump. The Cu(II)/**1** system was studied by titrating a Cu(II) solution (4.5×10^{-3} M) with the **1** solution. No KCl or KNO_3 was added to the solution in order to avoid precipitation of insoluble complexes. Thirty spectra were collected (Cu/Ligand up to 1/2.2) in the calculated pH range 1.3−2.9. Formation of insoluble Ag^+/**1** complexes at the liquid junction hampered a direct pH measurement. The Cu(II)/**3** and Cu(II)/**5** systems were studied at $I = 0.1$ M (KCl) by titrating Cu(II) solutions (3 to 4×10^{-3} M) with **3** and **5** solutions and collecting 19 and 26 spectra, respectively (Cu/Ligand up to 1/2.3). The spectroscopic data were processed to calculate the global formation constants (log *β*) and the spectra of the complexes calculated by means of the program SPECFIT 32.[48] Distribution diagrams were calculated and plotted by the program HYSS.[49]

Cell Culture and Viability Assay. Human fibrosarcoma HT1080 cells and human liposarcoma SW872 cells were obtained from the Istituto Zooprofilattico Sperimentale (Brescia, Italy); HeLa cell line, derived from a human cervix carcinoma, was obtained from ATCC. Human foreskin fibroblasts (HF) were obtained as previously described.[50] Cells were all grown in Dulbecco's modified Eagle's medium (DMEM) supplemented with 10% fetal bovine serum (FBS), 4 mM glutamine, 100 U/mL penicillin, and 100 *μ*g/mL streptomycin. Cells were cultured at 37 °C in an atmosphere of 5% CO_2 in air, pH 7.4.

The cytotoxic effect of the various compounds was assessed with the resazurin assay as previously described.[23] Briefly, cells were seeded in complete growth medium in 96-well microplates at a density of 5×10^3 cells/well. Twenty four hours later the growth medium was substituted with fresh medium containing the drug to be tested at the selected concentration. After a further 48 h, cell viability was tested replacing medium with a solution of resazurin (44 *μ*M) in plain DMEM. After 2 h, the fluorescence was measured at 572 nm with a fluorimeter (Wallac 1420 Victor^2 Multilabel Counter, Perkin-Elmer).

Copper Uptake. HF, HeLa, HT1080, and SW872 cells (cell number ranging between 1 and 1.5×10^7) were left untreated (control) or treated for the indicated times with 25 *μ*M of **2** or $CuCl_2$, both dissolved in 0.1% DMSO. Cells were washed two times with cold PBS solution, and the cell suspension was collected with a rubber scraper. Cells were pelletted by centrifugation (800*g*, 15 min), resuspended in 1 mL of water (18 MΩ), and lysed by needle ultrasonication for 30 s. A small aliquot of lysate was used for protein quantification (Bio-Rad assay), while the remaining was diluted with 4 mL of concentrated HNO_3 and mineralized by a microwave procedure. The resulting cell lysates were analyzed for Cu content using ICP-AES (inductively coupled plasma atomic emission spectroscopy).

Fluorescent Probe for ROS Detection. For cell-free assay, H_2DCFDA was used as described elsewhere with minor modifications.[51] Briefly, H_2DCFDA was dissolved in DMSO at 1 mM, diluted to 100 *μ*M with 0.01 N NaOH to hydrolyze the ester function of the probe, and kept in the dark at room temperature for 30 min. The reaction was performed in a 96-well microplate adding to each well 10 *μ*L of the deesterified probe solution to 90 *μ*L of complete culture medium containing 25 *μ*M of **2**, 25 *μ*M $CuCl_2$, 100 *μ*M H_2O_2, or 25 *μ*M $CuCl_2$ + 100 *μ*M H_2O_2. The reaction was monitored for 120 min measuring fluorescence at 530 nm (λ_{exc} = 488 nm) with a fluorimeter (Wallac 1420 Victor^2 Multilabel Counter, Perkin-Elmer).

For cellular ROS determination,[37] HT1080 cells were plated in a 96-well plate at a density of 1.5×10^4 cells/well. The day after seeding growth medium was replaced with serum free fresh medium containing the same compounds used for the cell free system. After 12 h, cells were washed and incubated for 1 h with DMEM supplemented with 10 *μ*M H_2DCFDA or a 1 *μ*M C11-BODIPY. Cells were then washed twice with PBS, and the fluorescence was measured with a fluorimeter (for H_2DCFDA-loaded cells) or visualized with an inverted fluorescence Nikon microscope (for C11-BODIPY-loaded cells).

Glutathione Determination. Cell contents of total (GSx) and oxidized glutathione (GSSG) were determined with an enzymatic recycling assay based on the method of Griffith[52] adapted for microplates. HT1080 cells were plated in a 24-well plate (1.5×10^5 cell/well), and the day after seeding, the culture medium was

replaced with fresh medium in the absence or in the presence of 25 μM of **2**, 200 μM BSO, or 25 μM $CuCl_2$. After 3, 6, 9, or 12 h, cells were washed twice with PBS at 4 °C and glutathione was extracted for 30 min at 4 °C using a solution of 3% perchloric acid. Aliquots of the supernatants (100 μL) were transferred to a new 24-well plate and partially neutralized with 400 μL of a 0.125 M Na-phosphate buffer. An aliquot (150 μL) of the protein free supernatant was incubated for 60 min with 3 μL of 2-vinylpyridine at room temperature to achieve the complete derivatization of reduced glutathione (GSH). For GSx content determination, 40 μL of each specimen was transferred to a 96-well microplate and mixed with 160 μL of a solution containing 130 μL of 0.3 mM NADPH, 20 μL of 6 mM DTNB (5,5′-dithio-bis-nitrobenzoic acid), and 10 μL of 5 U/mL glutathione reductase. The absorbance at 405 nm was recorded after 4, 8, 16, and 20 min. GSSG determination was performed as described for GSx with the derivatized specimen. Two distinct standard curves for the two determinations were constructed using known concentrations of GSSG. The extracted cell monolayers were dried and finally dissolved with 0.5% sodium deoxycholate in 1 N NaOH for protein determination according to a modified Lowry procedure.[50]

Statistics. Dose−response curves were fitted with nonlinear regression (sigmoidal variable slope curve). IC_{50} values were calculated from the curves with GraphPad Prism 4.0. Student's *t*-test was used for statistical analysis with $P < 0.05$ considered statistically significant.

Acknowledgment. This work was supported by the Ministero dell'Istruzione, dell'Università e Ricerca (Rome, Italy) and by FIL, Università degli Studi di Parma. We are grateful to CIRCMSB (Consorzio Interuniversitario di Ricerca in Chimica dei Metalli nei Sistemi Biologici) and to Prof. Gian Carlo Gazzola for discussions and comments.

Supporting Information Available: HPLC determination of oxidized glutathione in cell lysates, electrochemistry of **2** and **4**, combustion analyses, and CIF of (**4**)·3/2H_2O, **6**, and **8**. This material is available free of charge via the Internet at http://pubs.acs.org.

References

(1) Rae, T. D.; Schmidt, P. J.; Pufahl, R. A.; Culotta, V. C.; O'Halloran, T. V. Undetectable intracellular free copper: the requirement of a copper chaperone for superoxide dismutase. *Science* **1999**, *284*, 805−808.
(2) Radisky, D.; Kaplan, J. Regulation of transition metal transport across the yeast plasma membrane. *J. Biol. Chem.* **1999**, *274*, 4481−4484.
(3) Wang. T.; Guo, Z. Copper in medicine: homeostasis, chelation therapy and antitumor drug design. *Curr. Med. Chem.* **2006**, *13*, 525−537.
(4) Uriu-Adams, J. Y.; Keen, C. L. Copper, oxidative stress, and human health. *Mol. Aspects Med.* **2005**, *26*, 268−298.
(5) Majumder, S.; Panda, G. S.; Choudhuri, S. K. Synthesis, characterization and biological properties of a novel copper complex. *Eur. J. Med. Chem.* **2003**, *38*, 893−898.
(6) Mookerjee, A.; Basu, J. M.; Majumder, S.; Chatterjee, S.; Panda, G. S.; Dutta, P.; Pal, S.; Mukherjee, P.; Efferth, T.; Roy. S.; Choudhuri, S. K. A novel copper complex induces ROS generation in doxorubicin resistant Ehrlich ascitis carcinoma cells and increases activity of antioxidant enzymes in vital organs in vivo. *BMC Cancer* **2006**, *6*, 267.
(7) Mookerjee, A.; Mookerjee Basu, J.; Dutta, P.; Majumder, S.; Bhattacharyya, S.; Biswas, J.; Pal, S.; Mukherjee, P.; Raha, S.; Baral, R. N.; Das, T.; Efferth, T.; Sa, G.; Roy, S.; Choudhuri, S. K. Overcoming drug-resistant cancer by a newly developed copper chelate through host-protective cytokine-mediated apoptosis. *Clin. Cancer Res.* **2006**, *12*, 4339−4349.
(8) Valko, M.; Rhodes, C. J.; Moncol, J.; Izakovic, M.; Mazur, M. Free radicals, metals and antioxidants in oxidative stress-induced cancer. *Chem. Biol. Interact.* **2006**, *160*, 1−40.
(9) Estrela, J. M.; Ortega, A.; Obrador, E. Glutathione in cancer biology and therapy. *Crit. Rev. Clin. Lab. Sci.* **2006**, *43*, 143−181.
(10) Easmon, J.; Purstinger, G.; Heinisch, G.; Roth, T.; Fiebig, H. H.; Holzer, W.; Jager, W.; Jenny, M.; Hofmann, J. Synthesis, cytotoxicity, and antitumor activity of copper(II) and iron(II) complexes of (4)N-azabicyclo[3.2.2]nonane thiosemicarbazones derived from acyl diazines. *J. Med. Chem.* **2001**, *44*, 2164−2171.
(11) Afrasiabi, Z.; Sinn, E.; Chen, J.; Ma, Y.; Rheingold, A. L.; Zakharov, L. N.; Rath, N.; Padhye, S. Appended 1,2-naphthoquinones as anticancer agents 1: synthesis, structural, spectral and antitumor activities of ortho-naphthaquinone thiosemicarbazone and its transition metal complexes. *Inorg. Chim. Acta* **2004**, *357*, 271−278.
(12) Ferrari, M. B.; Fava, G. G.; Leporati, E.; Pelosi, G.; Rossi, R.; Tarasconi, P.; Alberini, R.; Bonati, A.; Lunghi, P.; Pinelli, S. Synthesis, characterisation and biological activity of three copper (II) complexes with a modified nitrogenous base: 5-formyluracil thiosemicarbazone. *J. Inorg. Biochem.* **1998**, *70*, 145−154.
(13) Ferrari, M. B.; Bisceglie, F.; Pelosi, G.; Sassi, M.; Tarasconi, P.; Cornia, M.; Capacchi, S.; Alberini, R.; Pinelli, S. Synthesis, characterization and X-ray structures of new antiproliferative and proapoptotic natural aldehyde thiosemicarbazones and their nickel(II) and copper(II) complexes. *J. Inorg. Biochem.* **2002**, *90*, 113−126.
(14) Cerchiaro, G.; Aquilano, K.; Filomeni, G.; Rotilio, G.; Circolo, M. R.; da Costa Ferriera, A. M. Isatin-Schiff base copper(II) complexes and their influence on cellular viability. *J. Inorg. Biochem.* **2005**, *99*, 1433−1440.
(15) Tonde, S. S.; Kumbhar, A. S.; Padhye, S. B.; Butcher, R. J. Self-activating nuclease activity of copper (II) complexes of hydroxyl-rich ligands. *J. Inorg. Biochem.* **2006**, *100*, 51−57.
(16) Raper, E. Copper complexes of heterocyclic thioamides and related ligands. *Coord. Chem. Rev.* **1994**, *129*, 91−156.
(17) Velayutham, M.; Villamena, F. A.; Navamal, M.; Fishbain, J. C.; Zweier, L. Z. Glutathione-mediated formation of oxygen free radicals by the major metabolite of oltipraz. *Chem. Res. Toxicol.* **2005**, *18*, 970−975.
(18) Epe, B.; Ballmeier, D.; Adam, W.; Grimm, G. N.; Saha-Moller, C. R. Photolysis of N-hydroxypyridinethiones: a new source of hydroxyl radicals for the direct damage of cell-free and cellular DNA. *Nucleic Acids Res.* **1996**, *24*, 1625−1631.
(19) Moller, M.; Adam, W.; Saha-Moller, C. R.; Stopper, H. Studies on cytotoxic and genotoxic effects of N-hydroxypyridine-2-thione (Omadine) in L5178Y mouse lymphoma cells. *Toxicol. Lett.* **2002**, *136*, 77−84.
(20) Adsule, S.; Barve, V.; Chen, D.; Ahmed, F.; Dou, Q. P.; Padhye, S.; Sarkar, F. H. Novel schiff base copper complexes of quinoline-2. carboxaldehyde as proteasome inhibitors in human prostate cancer cells. *J. Med. Chem.* **2006**; *49*, 7242−7246.
(21) Chen, D.; Cui, Q. C.; Yang, H.; Dou, Q. P. Disulfiram, a clinically used anti-alcoholism drug and copper-binding agent, induces apoptotic cell death in breast cancer cultures and xenografts via inhibition of the proteasome activity. *Cancer Res.* **2006**, *66*, 10425−10433.
(22) Dallavalle, F.; Gaccioli, F.; Franchi-Gazzola, R.; Lanfranchi, M.; Marchiò, L.; Pellinghelli, M. A.; Tegoni, M. *J. Inorg. Biochem.* Synthesis, molecular structure, solution equilibrium, and antiproliferative activity of thioxotriazoline and thioxotriazole complexes of copper II and palladium II. **2002**, *92*, 95−104.
(23) Tardito, S.; Bussolati, O.; Gaccioli, F.; Gatti, R.; Guizzardi, S.; Uggeri, J.; Marchiò, L.; Lanfranchi, M.; Franchi-Gazzola, R. Non-apoptotic programmed cell death induced by a copper(II) complex in human fibrosarcoma cells. *Histochem. Cell Biol.* **2006**, *126*, 473−482.
(24) Cummings, B. S.; Schnellmann, R. G. Cisplatin-induced renal cell apoptosis: caspase 3-dependent and -independent pathways. *J. Pharmacol. Exp. Ther.* **2002**, *302*, 8−17.
(25) Kolenko, V. M.; Uzzo, R. G.; Bukowski, R.; Finke, J. H. Caspase-dependent and -independent death pathways in cancer therapy. *Apoptosis* **2000**, *5*, 17−20.
(26) Clarke, M. J.; Zhu, F.; Frasca, D. R. Non-Platinum Chemotherapeutic Metallopharmaceuticals. *Chem. Rev.* **1999**, *99*, 2511−2533.
(27) Clarke, M. J. Ruthenium metallopharmaceuticals. *Coord. Chem. Rev.* **2003**, *236*, 209−233.
(28) Huang, R.; Wallquist, A.; Covell, D. J. Anticancer metal compounds in NCI's tumor-screening database: putative mode of action. *Biochem. Pharm.* **2005**, *69*, 1009−1039.
(29) Gaccioli, F.; Franchi-Gazzola, R.; Lanfranchi, M.; Marchiò, L.; Metta, G.; Pellinghelli, M. A.; Tardito, S.; Tegoni, M. Synthesis, solution equilibria and antiproliferative activity of copper(II) aminomethyltriazole and aminomethylthioxotriazoline complexes. *J. Inorg. Biochem.* **2005**, *99*, 1573−1584.
(30) Gomez-Saiz, P.; Garc_a-Tojal, J.; Maestro, M. A.; Arnaiz, F. J.; Rojo, T. Evidence of desulfurization in the oxidative cyclization of thiosemicarbazones. Conversion to 1,3,4-oxadiazole derivatives. *Inorg. Chem.* **2002**, *41*, 1345−1347.
(31) Gómez-Saiz, P.; Gil-García, R.; Maestro, M. A.; Pizarro, J. L.; Arriortua, M. I.; Lezama, L.; Rojo, T.; García-Tojal, J. Unexpected Behaviour of Pyridine-2-carbaldehyde Thiosemicarbazonatocopper(II) Entities in Aqueous Basic Medium - Partial Transformation of Thioamide into Nitrile. *Eur. J. Inorg. Chem.* **2005**, *17*, 3409−3413.

(32) Lopez-Torres, E.; Mendiola, M. A.; Pastor, C. Crystal structures of triazine-3-thione derivatives by reaction with copper and cobalt salts. *J. Inorg. Chem.* **2006**, *45*, 3103−3112.
(33) Bigoli, F.; Lanfranchi, M.; Pellinghelli, M. A. Synthesis and Crystal Structures of 4-Amino-3-methyl-1,4-dihydro-1,2,4-triazole-5-thione, Dichloro(4-amino-3-methyl-1,4-dihydro-1,2,4-triazole-5-thione)copper(II) Monohydrate, and *catena*-Di-μ-(4-amino-3-methyl-1,2,4-triazole-N^1,N^2)copper(II). An example of Desulphuration promoted by Copper(II). *J. Chem. Res. (S)* **1990**, 214−215.
(34) According to ref 18, the pK_a value of the pyridyl group of **1** is 1.94-(1).
(35) Clarke, P. G. Developmental cell death: morphological diversity and multiple mechanisms. *Anat. Embryol.* **1990**, *181*, 195−213.
(36) Ribas, J.; Bettayeb, K.; Ferandin, Y.; Knockaert, M.; Garrofe-Ochoa, X.; Totzke, F.; Schachtele, C.; Mester, J.; Polychronopoulos, P.; Magiatis, P.; Skaltsounis, A. L.; Boix, J.; Meijer, L. 7-Bromoindirubin-3′-oxime induces caspase-independent cell death. *Oncogene* **2006**, *25*, 6304−6318.
(37) Orhan, H.; Gurer-Orhan, H.; Vriese, E.; Vermeulen, N. P.; Meerman, J. H. Application of lipid peroxidation and protein oxidation biomarkers for oxidative damage in mammalian cells. A comparison with two fluorescent probes. *Toxicol. In Vitro* **2006**, *20*, 1005−1013.
(38) Griffith, O. W. Biologic and pharmacologic regulation of mammalian glutathione synthesis. *Free Radic. Biol. Med.* **1999**, *27*, 922−935.
(39) Griffith, O. W.; Meister, A. Potent and specific inhibition of glutathione synthesis by buthionine sulfoximine (S-n-butyl homocysteine sulfoximine). *J. Biol. Chem.* **1979**, *254*, 7558−7560.
(40) Ueda, S.; Nakamura, H.; Masutani, H.; Sasada, T.; Yonehara, S.; Takabayashi, A.; Yamaoka, Y.; Yodoi, J. Redox regulation of caspase-3(-like) protease activity: regulatory roles of thioredoxin and cytochrome c. *J. Immunol.* **1998**, *161*, 6689−6695.
(41) Xin Zhang, C; Lippard, S. J. New metal complexes as potential therapeutics. *Curr. Opin. Chem. Biol.* **2003**, *7*, 481−489.
(42) Walker, N.; Stuart, D. An empirical method for correcting diffractometer data for absorption effects. *Acta Crystallogr.* **1983**, *A39*, 158−166.
(43) Altomare, A.; Burla, M. C.; Camalli, M.; Cascarano, G. L.; Giacovazzo, C.; Guagliardi, A.; Moliterni, A. G. G.; Polidori, G.; Spagna, R. SIR97: a new tool for crystal structure determination and refinement. *J. Appl. Crystallogr.* **1999**, *32*, 115.
(44) Sheldrick, G. M.; SHELX97. Programs for Crystal Structure Analysis (1997) (Release 97-2). University of Göttingen, Germany.
(45) Farrugia, L. J. WinGX Suite for small-molecule single-crystal crystallography. *J. Appl. Crystallogr.* **1999**, *32*, 837.
(46) Farrugia, L. J. ORTEP-3 for Windows - a version of ORTEP-III with a Graphical User Interface (GUI). *J. Appl. Crystallogr.* **1997**, *30*, 565.
(47) Dallavalle, F.; Folesani, G.; Marchelli, R.; Galaverna, G. Stereoselective Formation of Ternary Copper(II) Complexes of (*S*)-amino-acid amides and (*R*)- or (*S*)-amino acids in aqueous solution. *Helv. Chim. Acta* **1994**, *77*, 1623−1630.
(48) Binstead, R. A.; Jung, B.; Zuberbühler, A. D. SPECFIT Global Analysis System, Version 3.0, Spectrum Software Associates, Marlborough, MA, 2004.
(49) Alderighi, L.; Gans, P.; Ienco, A.; Peters, D.; Sabatini, A.; Vacca, A. Hyperquad simulation and speciation (HySS): a utility program for the investigation of equilibria involving soluble and partially soluble species. *Coord. Chem. Rev.* **1999**, *184*, 311−318.
(50) Gazzola, G. C.; Dall'Asta, V.; Franchi-Gazzola, R.; White, M. F. The cluster-tray method for rapid measurement of solute fluxes in adherent cultured cells. *Anal. Biochem.* **1981**, *115*, 368−374.
(51) Myhreab, O.; Andersen, J. M.; Aarnesc, H.; Fonnum, F. Evaluation of the probes 2′,7′-dichlorofluorescin diacetate, luminol, and lucigenin as indicators of reactive species formation. *Biochem. Pharm.* **2003**, *65*, 1575−1582.
(52) Griffith, O. W. Determination of glutathione and glutathione disulfide using glutathione reductase and 2-vinylpyridine. *Anal. Biochem.* **1980**, *106*, 207−212.

JM061174F